Transient beam loading and rf power evaluation for future circular colliders

Ivan Karpov* and Philippe Baudrenghien
CERN, Geneva 1211, Switzerland

(Received 11 February 2019; published 6 August 2019)

Interaction of the beam with the fundamental impedance of the accelerating cavities can limit the performance of high-current accelerators. It can result in a significant variation of bunch-by-bunch parameters (bunch length, synchronous phase, etc.) if filling patterns contain gaps that are not negligible compared with the cavity filling time. In the present work, this limitation is analyzed using the steady-state time-domain approach for the high-current option (Z) of the future circular electron-positron collider and for the future circular hadron-hadron collider. Mitigation of transient beam loading by direct rf feedback is addressed with evaluation of additional required generator power.

DOI: 10.1103/PhysRevAccelBeams.22.081002

I. INTRODUCTION

The future circular electron-positron collider (FCC-ee) [1] as a predecessor of the future circular hadron-hadron collider (FCC-hh) [2] is considered to be built in five energy stages, defined by the physics program. To keep the same power loss budget for the synchrotron radiation in FCC-ee, the beam current will be gradually reduced from 1.4 A to 5.4 mA as the beam energy increases from 45.6 GeV (the Z pole) to 182.5 GeV (the $t\bar{t}$ threshold), respectively. The high current colliders, the FCC-hh and the FCC-ee Z, with parameters summarized in Table I, will have filling patterns with gaps that are not negligible compared with the cavity filling time. Thus, they will suffer from transient beam loading issues which can result in modulation of the cavity voltage and beam parameters. For example, change of the cavity voltage phase produced by a partly filled ring will cause a significant phase error for newly injected bunch trains. In the hadron machine this could result in additional emittance blowup after filamentation as well as possible particle losses. Modulation of synchronous phase can result in a collision point shift and reduce luminosity due to the presence of a finite crossing angle and a potential contribution of the hourglass effect. This limitation can be eliminated by matching gap transients which requires the collider rings to have identical filling patterns, rf systems, and total beam currents. If there is a large bunch length spread due to modulation of the cavity voltage, for the shortest proton bunches Landau damping can be lost as it is proportional to the fifth power of the bunch length [3]. This makes these bunches potentially unstable.

In general, there are two methods to analyze the beam-induced transients: in frequency domain and time domain. The former, developed by Pedersen [5], is usually called a small-signal model. It allows one to calculate the modulation of cavity voltage produced by modulation of the beam current and it was applied for the earlier set of the FCC-ee Z parameters in [6]. The latter method is the tracking of the beam and the simulation of the rf system evolution in the time domain [7,8] which converges to the steady-state regime after many synchrotron periods. Considering a machine with large circumference, high beam current, and large number of bunches, as for the case of high-current future circular colliders, an analytical

TABLE I. The parameters of high-intensity high-luminosity colliders used for calculations in this work [1,2,4].

Parameter	Units	FCC-ee Z	FCC-hh (injection/physics)
Circumference, C	km		97.75
Harmonic number, h			130680
rf frequency, f_{rf}	MHz		400.79
(R/Q)	Ω		42.3
Beam energy, E	TeV	0.0456	3.3/50
dc beam current, $I_{b,\mathrm{dc}}$	A	1.39	0.52
Number of bunches per beam, M		16640	10400
Bunch population, N_p	10^{11}	1.7	1.0
rms bunch length, σ	ps	40	338/267
Momentum compaction factor, α_p	10^{-6}	14.79	101.35
Total rf voltage, V_{tot}	MV	100	12/38
Number of cavities, N_{cav}		52	24
Energy loss per turn, U_0	MeV	36	0/4.67

*ivan.karpov@cern.ch

model, which does not assume the small cavity voltage modulation, may have an advantage for calculations of the beam-induced transients.

In this work, we present analytical results of beam loading in superconducting rf cavities modeled by a lumped circuit with a generator linked to the cavity via a circulator [9]. We consider cavity voltage, beam and generator current as complex phasors. This approach was successfully used to derive a power saving algorithm in the large hadron collider (LHC) [10]. It allows us to get a steady-state solution for beam and cavity parameters (beam phase, cavity voltage amplitude, and phase) for arbitrary beam currents and filling schemes. In Sec. II we describe the steady-state time-domain approach. For the case of constant generator current we derive the system of equations to compute modulations of the beam and cavity parameters in Sec. II A and then briefly discuss optimal parameters for which the generator power is minimized. The equations of the frequency-domain analysis are obtained from the linearized model in Sec. II A 2. The approach that keeps the cavity voltage amplitude constant for an arbitrary synchronous phase is discussed in Sec. II B. Mitigation schemes of the beam and cavity parameter modulations using the direct rf feedback around the cavity are presented in Sec. III. Section IV contains the main results of the transient beam loading analysis for FCC-ee Z and FCC-hh. Finally, Sec. V summarizes the main results.

II. TRANSIENT BEAM LOADING

In operation of the Z machine different filling schemes can be used. To perform systematic analysis of the transient beam loading, we introduce the filling schemes presented in [11] and schematically shown in Fig. 1. We consider a beam containing M bunches, which can be grouped in n_{tr} equal trains with a distance between the first bunches of the consecutive trains t_{tt}. This distance should be a multiple of the bunch spacing t_{bb}. Each train contains a number of filled buckets $M_b \leq t_{\mathrm{tt}}/t_{\mathrm{bb}}$. The beam has a regular filling, which can also contain an abort gap of length t_{gap}. Thus, the dc beam current depends on the filling scheme $I_{b,\mathrm{dc}} = n_{\mathrm{tr}} M_b N_p e/t_{\mathrm{rev}}$, with e the elementary charge, t_{rev} the revolution period, and N_p the number of particles per bunch.

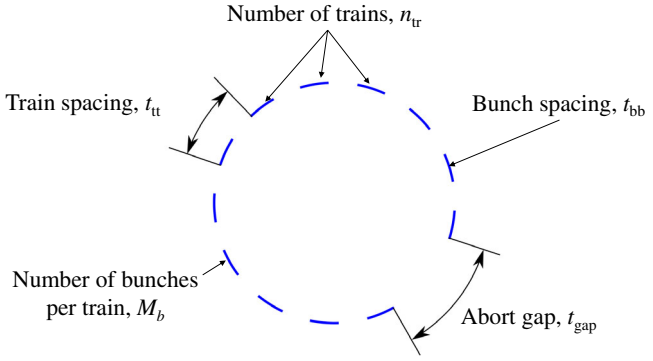

FIG. 1. Sketch of the filling schemes used for the present study.

For a given filling scheme, the abort gap length can be calculated as

$$t_{\mathrm{gap}} = \frac{t_{\mathrm{rev}}}{n_{\mathrm{gap}}} - \left[\left(\frac{n_{\mathrm{tr}}}{n_{\mathrm{gap}}} - 1\right) t_{\mathrm{tt}} + M_b t_{\mathrm{bb}}\right] + t_{\mathrm{bb}} - t_{\mathrm{rf}}, \quad (1)$$

where n_{gap} is the number of abort gaps, $t_{\mathrm{rf}} = 1/f_{\mathrm{rf}}$, and f_{rf} is the rf frequency. In FCC-hh, $f_{\mathrm{rf}} t_{\mathrm{bb}} = 10$, $M_b = 80$ is defined by machine protection requirements, and $f_{\mathrm{rf}} t_{\mathrm{tt}} = 980$ is given by the injection kicker rise time. To prevent damage of accelerator components due to an asynchronous beam dump caused by erratic firing of the extraction kicker, the filling scheme with four distributed abort gaps is considered to be used in operation [12]. In total $n_{\mathrm{tr}} = 130$ trains will circulate in the machine.

The gaps in the filling pattern generate a modulation of the cavity voltage. Past work [9] based on the lumped circuit model (Fig. 2), has derived the differential equation for transient beam loading coming from beam-to-fundamental mode interaction:

$$I_g(t) = \frac{V(t)}{2(R/Q)}\left(\frac{1}{Q_L} - 2i\frac{\Delta\omega}{\omega_{\mathrm{rf}}}\right) + \frac{dV(t)}{dt}\frac{1}{\omega_{\mathrm{rf}}(R/Q)} + \frac{I_{b,\mathrm{rf}}(t)}{2}, \quad (2)$$

where I_g is the generator current, V is the cavity voltage, $I_{b,\mathrm{rf}}$ is the rf component of the beam current, (R/Q) is the ratio of the shunt impedance to the quality factor of the cavity fundamental mode expressed in circuit ohm, $\Delta\omega = \omega_0 - \omega_{\mathrm{rf}}$ is the cavity detuning, ω_0 is the cavity resonant frequency, and $\omega_{\mathrm{rf}} = 2\pi f_{\mathrm{rf}}$ is the rf angular frequency. The loaded quality factor $1/Q_L = 1/Q_{\mathrm{ext}} + 1/Q_0$ is calculated from the cavity quality factor Q_0 and the coupler quality factor $Q_{\mathrm{ext}} = Z_c/(R/Q)$ defined by the line impedance transformed at the gap by the main coupler with impedance Z_c. Considering a superconducting cavity with $Q_0 \gg Q_{\mathrm{ext}}$, the generator power can be written as [9]

$$P(t) = \frac{1}{2}(R/Q)Q_{\mathrm{ext}}|I_g(t)|^2 \approx \frac{1}{2}(R/Q)Q_L|I_g(t)|^2. \quad (3)$$

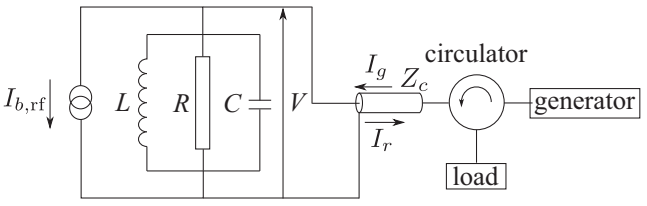

FIG. 2. The lumped circuit model: a cavity is modeled by an LCR block, the coupler by a connected transmission line of impedance Z_c, and the beam by a current source. $I_{b,\mathrm{rf}}$ is the rf component of the beam current, I_g is the generator current, and I_r is the reflected current, which is absorbed in the matched load (the generator is connected to the cavity via a circulator).

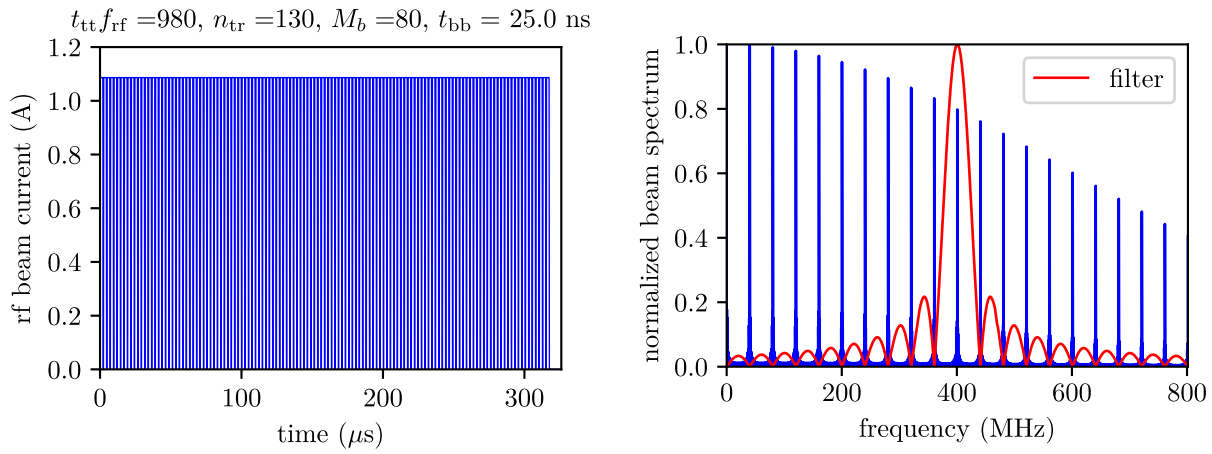

FIG. 3. Left: an example of the amplitude of the rf component of the beam current within one turn for FCC-hh filling scheme with a single abort gap. Right: corresponding amplitude of the beam spectrum (blue) and the amplitude of the filter function (red).

In reality the rf power chain (amplifier, circulator, etc.) has limited bandwidth and cannot track fast bunch-by-bunch variation of the beam current. In the present work, the rf beam current amplitude $A_b(t)$ is a stepwise function $u(t)$ with a sampling time $t_{\rm rf}$. The value of the stepwise function in an mth rf bucket is $u(mt_{\rm rf}) = A_{b,\rm peak}$ for $m = k + n$, where $k \in [0, t_{\rm bb}/t_{\rm rf} - 1]$, n is the index of the rf bucket filled with bunches, and $u(mt_{\rm rf}) = 0$ otherwise (see the left-hand plot in Fig. 3). Here, $A_{b,\rm peak} = |F_b|eN_p/t_{\rm bb}$ is the peak rf beam current amplitude averaged over a window of length $t_{\rm bb}$ with the complex form factor [13]

$$F_b = 2\frac{\mathcal{F}[\lambda(t)]_{\omega=\omega_{\rm rf}}}{\mathcal{F}[\lambda(t)]_{\omega=0}} \tag{4}$$

obtained as the ratio of the Fourier transform of the bunch density distribution λ at the rf frequency to the one at dc. It depends on the particle distribution function, which is described in the Appendix. This rf beam current representation is equivalent to filtering of the beam spectrum with a function centered at $f_{\rm rf}$ and having zeros at all other $1/t_{\rm bb}$ harmonics (see the right-hand plot in Fig. 3), which is also done in the LHC.

Equation (2) links the cavity voltage to the beam and generator current. If we set the generator current constant, we can calculate the beam induced modulation of the cavity voltage. If, on the other hand, we impose a constant voltage (full compensation of the transient beam loading), the equation indicates that the generator current must follow the beam current modulation. This can lead to a significant increase in required power, depending on parameters such as cavity detuning and loaded quality factor. The above two strategies are discussed in the following sections.

A. Case of constant generator current

The generator current remains constant and there is no attempt to compensate the transient beam loading. For calculations of the beam induced transients, we assume modulations of the cavity voltage and the beam current in the form

$$V(t) = A(t)e^{i\phi(t)}, \qquad I_{b,\rm rf}(t) = A_b(t)e^{-i\phi_s + i\phi_b(t)}, \tag{5}$$

with A the cavity voltage amplitude, and ϕ the modulation of the cavity voltage phase. The average beam stable phase ϕ_s (referred as the synchronous phase below) can be found as the phase of the complex form factor $F_b = |F_b|e^{-i\phi_s}$ (see the Appendix). The modulation of the beam phase ϕ_b should satisfy the following relation:

$$A(t)\cos\left[\phi_s - \phi_b(t) + \phi(t)\right] = V_{\rm cav}\cos\phi_s, \tag{6}$$

where $V_{\rm cav} = V_{\rm tot}/N_{\rm cav}$ is the average cavity voltage, $V_{\rm tot}$ is the total rf voltage, and $N_{\rm cav}$ is the number of rf cavities. Substituting Eq. (5) in Eq. (2) and separating real and imaginary parts, we get the following system of equations:

$$\frac{dA(t)}{dt} = -\frac{A(t)}{\tau} + (R/Q)\omega_{\rm rf} \times \left\{ I_{g,c}\cos[\phi_L - \phi(t)] - \frac{A_b(t)\cos[\phi_s - \phi_b(t) + \phi(t)]}{2} \right\}, \tag{7}$$

$$\frac{d\phi(t)}{dt} = \Delta\omega + \frac{(R/Q)\omega_{\rm rf}}{A(t)} \times \left\{ I_{g,c}\sin[\phi_L - \phi(t)] + \frac{A_b(t)\sin[\phi_s - \phi_b(t) + \phi(t)]}{2} \right\}, \tag{8}$$

with the cavity filling time $\tau = 2Q_L/\omega_{\rm rf}$. The constant generator current amplitude $I_{g,c}$, and the loading angle ϕ_L that is the phase of the generator current with respect to the average cavity voltage can be calculated by averaging Eq. (2) over one turn

$$
\begin{aligned}
I_{g,c}e^{i\phi_L} &= \frac{1}{t_{\mathrm{rev}}}\int_t^{t+t_{\mathrm{rev}}} I_g(u)du \\
&= \frac{1}{t_{\mathrm{rev}}}\int_t^{t+t_{\mathrm{rev}}}\left[\frac{V(u)}{2(R/Q)}\left(\frac{1}{Q_L}-2i\frac{\Delta\omega}{\omega_{\mathrm{rf}}}\right)\right. \\
&\quad \left.+\frac{dV(u)}{du}\frac{1}{\omega_{\mathrm{rf}}(R/Q)}+\frac{I_{b,\mathrm{rf}}(u)}{2}\right]du \\
&= \frac{V_{\mathrm{cav}}}{2(R/Q)}\left(\frac{1}{Q_L}-2i\frac{\Delta\omega}{\omega_{\mathrm{rf}}}\right)+\frac{\langle I_{b,\mathrm{rf}}\rangle}{2}, \qquad (9)
\end{aligned}
$$

where we use the fact that in the steady-state situation the cavity voltage is a periodic function $V(t+t_{\mathrm{rev}})=V(t)$, and the average rf harmonic of the beam current is

$$
\langle I_{b,\mathrm{rf}}\rangle = \frac{1}{t_{\mathrm{rev}}}\int_t^{t+t_{\mathrm{rev}}} I_{b,\mathrm{rf}}(u)du = |F_b|I_{b,\mathrm{dc}}e^{-i\phi_s}. \qquad (10)
$$

Unfortunately Eqs. (6), (7), (8) can not be solved analytically, but the results of numerical calculations will be presented in Sec. IV.

1. Optimal parameters

The generator power is constant for the case of constant generator current and can be expressed using Eqs. (3), (9), (10) as

$$
\begin{aligned}
P_{g,c} &= \frac{1}{2}(R/Q)Q_L|I_{g,c}|^2 \\
&= \frac{1}{2}(R/Q)Q_L\left\{\left[\frac{V_{\mathrm{cav}}}{2(R/Q)Q_L}+\frac{|F_b|I_{b,\mathrm{dc}}\cos\phi_s}{2}\right]^2\right. \\
&\quad \left.+\left[\frac{V_{\mathrm{cav}}}{(R/Q)}\frac{\Delta\omega}{\omega_{\mathrm{rf}}}+\frac{|F_b|I_{b,\mathrm{dc}}\sin\phi_s}{2}\right]^2\right\}. \qquad (11)
\end{aligned}
$$

Setting the partial derivative of the average generator power with respect to $\Delta\omega$ to zero we get the optimal cavity detuning

$$
\Delta\omega_{\mathrm{opt}} = -\omega_{\mathrm{rf}}\frac{|F_b|I_{b,\mathrm{dc}}(R/Q)\sin\phi_s}{2V_{\mathrm{cav}}}. \qquad (12)
$$

The optimal loaded quality factor that minimizes $P_{g,c}$ for $\Delta\omega=\Delta\omega_{\mathrm{opt}}$ is

$$
Q_{L,\mathrm{opt}} = \frac{V_{\mathrm{cav}}}{(R/Q)|F_b|I_{b,\mathrm{dc}}\cos\phi_s}, \qquad (13)
$$

and the optimal generator power is

$$
P_{g,\mathrm{opt}} = \frac{V_{\mathrm{cav}}|F_b|I_{b,\mathrm{dc}}\cos\phi_s}{2}. \qquad (14)
$$

For the optimal parameters, however, the beam is unstable because the second Robinson limit [14] is reached, which reads as

$$
Y < -\frac{2\sin\phi_s}{\sin(2\phi_z)}. \qquad (15)
$$

When no loop around the cavity is present, with $Y=|F_b|I_{b,\mathrm{dc}}(R/Q)Q_L/V_{\mathrm{cav}}$ the relative beam loading [15], and the detuning angle ϕ_z is defined as $\tan\phi_z=2Q_L\Delta\omega/\omega_{\mathrm{rf}}$. In this case $Y=1/\cos\phi_s$ and $\phi_z=-\phi_s$, so Eq. (15) is not satisfied.

2. Linearized model (frequency domain calculations)

To linearize Eqs. (6)–(8) we define the normalized modulations of the beam current amplitude a_b and the cavity voltage amplitude a_V

$$
A_b(t)=|F_b|I_{b,\mathrm{dc}}[1+a_b(t)], \qquad A(t)=V_{\mathrm{cav}}[1+a_V(t)] \qquad (16)
$$

and assume $|a_V|\ll 1$, $|\phi|\ll 1$ and $|\phi_b|\ll 1$, while $|a_b|$ could be 100% modulated. The linearized system of equations is

$$
\begin{aligned}
\frac{da_V(t)}{dt} &= -\left(\frac{1}{\tau}+\frac{\Delta\omega_{\mathrm{opt}}}{\tan\phi_s}\right)a_V(t)+(\Delta\omega_{\mathrm{opt}}-\Delta\omega)\phi(t) \\
&\quad +\frac{a_b(t)\Delta\omega_{\mathrm{opt}}}{\tan\phi_s}, \qquad (17)
\end{aligned}
$$

$$
\begin{aligned}
\frac{d\phi(t)}{dt} &= \left(\Delta\omega-\frac{\Delta\omega_{\mathrm{opt}}}{\tan^2\phi_s}\right)a_V(t)-\left(\frac{1}{\tau}-\frac{\Delta\omega_{\mathrm{opt}}}{\tan\phi_s}\right)\phi(t) \\
&\quad -a_b(t)\Delta\omega_{\mathrm{opt}}, \qquad (18)
\end{aligned}
$$

$$
\phi_b(t)=\phi(t)-\frac{a_V(t)}{\tan\phi_s}. \qquad (19)
$$

Then applying a Laplace transformation we obtain the transfer functions from the beam current amplitude to the cavity voltage amplitude, the cavity voltage phase, and the beam phase:

$$
\frac{\tilde{a}_V}{\tilde{a}_b} = -\frac{\Delta\omega_{\mathrm{opt}}}{D(s)}\left[\frac{\Delta\omega_{\mathrm{opt}}}{\sin^2\phi_s}-\Delta\omega-\left(s+\frac{1}{\tau}\right)\cot\phi_s\right], \qquad (20)
$$

$$
\frac{\tilde{\phi}}{\tilde{a}_b} = -\frac{\Delta\omega_{\mathrm{opt}}}{D(s)}\left[\left(\frac{\Delta\omega_{\mathrm{opt}}}{\sin^2\phi_s}-\Delta\omega\right)\cot\phi_s+\left(s+\frac{1}{\tau}\right)\right], \qquad (21)
$$

$$
\frac{\tilde{\phi}_b}{\tilde{a}_b} = -\frac{\Delta\omega_{\mathrm{opt}}}{D(s)\sin^2\phi_s}\left(s+\frac{1}{\tau}\right), \qquad (22)
$$

where

$$
D(s)=\left(s+\frac{1}{\tau}\right)^2-\Delta\omega\left[\frac{\Delta\omega_{\mathrm{opt}}}{\sin^2\phi_s}-\Delta\omega\right], \qquad (23)
$$

and $\tilde{a}$ is the Laplace image of the variable a. Equations (20) and (21) are identical to Eqs. (13) and (14) in Ref. [16] with

the substitution $\phi_B = \pi/2 + \phi_s$ as we use the electron machine convention. For a detuning slightly larger than optimal [Eq. (12)] $\Delta\omega_m = \Delta\omega_{\rm opt}/\sin^2\phi_s$, which is called the "magic" detuning [17], and simple first order responses can be obtained from Eqs. (20)–(22)

$$\frac{\tilde{a}_V}{\tilde{a}_b} = -\frac{\Delta\omega_{\rm opt}\tau\cot\phi_s}{1+\tau s}, \qquad \frac{\tilde{\phi}}{\tilde{a}_b} = -\frac{\Delta\omega_{\rm opt}\tau}{1+\tau s},$$
$$\frac{\tilde{\phi}_b}{\tilde{a}_b} = \frac{\Delta\omega_m\tau}{1+\tau s}. \tag{24}$$

This magic detuning is used in the following calculations, because for the optimal detuning and optimal loaded quality factor the beam is unstable as was discussed above. This results in an increase of power consumption by a factor $1 + 1/(2\tan\phi_s)^2$, which is about 1.025 for the FCC-ee parameters.

If the cavity filling time is significantly longer than the beam gaps, the modulation of cavity voltage (amplitude and phase) and beam phase will be almost linear in the beam gaps. We propose to use the following equations to estimate the peak-to-peak beam phase modulation:

$$\max\phi_b - \min\phi_b = |\Delta\omega_m t_{\rm gap}|, \tag{25}$$

and peak-to-peak phase modulation of the cavity voltage

$$\max\phi - \min\phi = |\Delta\omega_{\rm opt} t_{\rm gap}|, \tag{26}$$

which can be obtained from transfer functions in Eq. (24) assuming a step excitation due to the abort gap. The latter equation was originally proposed in Ref. [18] for the case of optimum cavity detuning.

B. Case of constant cavity voltage amplitude

The shift in collision point (z-vertex) due to beam phase modulation can be mitigated by a proper match of filling patterns, rf systems, and total beam currents. However, amplitude modulation of the cavity voltage can still affect bunch-by-bunch parameters (bunch length, longitudinal emittance, synchrotron frequency, etc.) and beam stability. Reference [10] proposes to keep constant the amplitude of the cavity voltage while allowing its phase modulation. This approach is currently used in the LHC where the stable phase is very close to $\pi/2$ (electron machine convention). The generator current amplitude is constant, while its phase is modulated. In the more general case ($\phi_s \neq \pi/2$) a similar scheme would require a significant amplitude modulation of the generator current as will be shown in this section.

If the cavity voltage amplitude remains constant, the beam phase modulation ϕ_b is at all time equal to the phase modulation of the cavity voltage ϕ [see Eq. (6)]. Assuming that the generator current is modulated in amplitude A_g and phase ϕ_g in the form $I_g(t) = A_g(t)e^{i\phi_g(t)}$, cavity voltage is $V(t) = V_{\rm cav}e^{i\phi(t)}$, and the rf component of the beam current $I_{b,\rm rf}(t) = A_b(t)e^{-i\phi_s + i\phi_b(t)} = A_b(t)e^{-i\phi_s + i\phi(t)}$, we rewrite Eq. (2),

$$A_g(t)e^{i\phi_g(t) - i\phi(t)} = \frac{V_{\rm cav}}{2(R/Q)Q_L} + \frac{A_b(t)\cos\phi_s}{2} - i\left[\frac{\Delta\omega V_{\rm cav}}{\omega_{\rm rf}(R/Q)} - \frac{V_{\rm cav}}{\omega_{\rm rf}(R/Q)}\frac{d\phi(t)}{dt} + \frac{A_b(t)\sin\phi_s}{2}\right]. \tag{27}$$

From Eq. (3) the instantaneous generator power in this case is

$$\begin{aligned} P(t) &= \frac{1}{2}(R/Q)Q_L|I_g(t)|^2 \\ &= \frac{1}{2}(R/Q)Q_L\left[\frac{V_{\rm cav}}{2(R/Q)Q_L} + \frac{A_b(t)\cos\phi_s}{2}\right]^2 \\ &\quad + \frac{1}{2}(R/Q)Q_L\left[\frac{\Delta\omega V_{\rm cav}}{\omega_{\rm rf}(R/Q)} - \frac{V_{\rm cav}}{\omega_{\rm rf}(R/Q)}\frac{d\phi(t)}{dt} + \frac{A_b(t)\sin\phi_s}{2}\right]^2. \end{aligned} \tag{28}$$

It can be minimized if the term in the second set of brackets equals zero. Using Eq. (12) the required phase modulation of the cavity voltage is

$$\phi(t) = -\frac{\Delta\omega_{\rm opt}}{|F_b|I_{b,\rm dc}}\int_{t_0}^{t} A_b(u)du + \Delta\omega(t - t_0) + \phi(t_0) \tag{29}$$

where $\phi(t_0)$ is an integration constant. In the steady-state situation $\phi(t + t_{\rm rev}) = \phi(t)$ and the beam current amplitude averaged over a turn is $|F_b|I_{b,\rm dc}$ [see Eq. (10)] resulting in the detuning being optimal $\Delta\omega = \Delta\omega_{\rm opt}$, similar to [10]. Thus the right-hand side of Eq. (27) becomes real and requires the generator current phase to be the same as the phase modulation of the cavity voltage ($\exp[i\phi_g(t) - i\phi(t)] = 1$). Also the generator current amplitude should follow the beam current modulation.

Finally, the peak generator power can be minimized for the loaded quality factor

$$Q_{L,\rm fd} = \frac{V_{\rm cav}}{(R/Q)A_{b,\rm peak}\cos\phi_s}, \tag{30}$$

and is given as

$$\begin{aligned} P_{g,\rm peak} &= \frac{V_{\rm cav}A_{b,\rm peak}\cos\phi_s}{2} = P_{g,\rm opt}\frac{A_{b,\rm peak}}{|F_b|I_{b,\rm dc}} \\ &= P_{g,\rm opt}\left[\frac{ht_{\rm rf}}{Mt_{\rm bb}}\right]. \end{aligned} \tag{31}$$

For the maximum bunch spacing available in operation, the ratio of the peak beam current amplitude to the average rf beam current is around one because bunches are more uniformly distributed in the ring. For the smallest bunch spacing ($t_{bb} = t_{rf}$), $h/M \gg 1$, and more generator power is required compared to the case without transient beam loading compensation.

This scheme is very attractive for hadron colliders ($\phi_s \approx \pi/2$) where the real valued term on the right-hand side of Eq. (27) can be reduced significantly by choosing a large Q_L resulting in low power consumption. In lepton colliders where ϕ_s differs from $\pi/2$, keeping voltage amplitude constant results in excessive required power. One must make a trade-off: accept "some" modulation of the cavity voltage within the available rf power budget.

III. COMPENSATION OF TRANSIENT BEAM LOADING

Partial compensation of the beam induced voltage modulation can easily be done using direct rf feedback around the cavity and amplifier (Fig. 4). This has been used in most high-intensity accelerators since the 1980s [19]. In addition to regulation of the cavity field in the presence of amplifier drifts and rf noise, it counteracts the longitudinal coupled-bunch instability driven by the fundamental cavity impedance Z_b [8,16,20]. The direct rf feedback reduces the cavity fundamental mode impedance seen by the beam such that the impedance of the closed loop is

$$Z_{cl}(\omega) = \frac{Z_b(\omega)}{1 + GZ_b(\omega)e^{-i\tau_d\omega + i\phi_{adj}}}, \tag{32}$$

where G is the feedback gain, τ_d is the overall loop delay, and ϕ_{adj} is the phase adjustment required to correctly set the feedback negative at the detuned cavity resonant frequency. The flat response is achieved and the feedback loop stability is guaranteed for $1/G = 2(R/Q)\omega_{rf}\tau_d$ [19]. In the presence of the direct rf feedback the generator current in Eq. (2) can be written as

$$I_g(t) = I_{g,c}e^{i\phi_L} + G[V_{ref}(t - \tau_d) - V(t - \tau_d)], \tag{33}$$

where $V_{ref}(t)$ is a reference signal whose shape depends on the compensation schemes discussed below. The constant offset $I_{g,c}e^{i\phi_L}$ in Eq. (33) guarantees the average cavity voltage amplitude to be equal V_{cav} for the finite value of the feedback gain G.

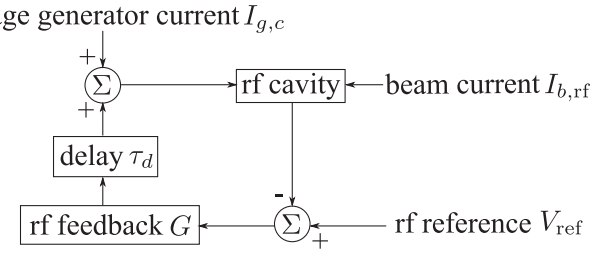

FIG. 4. The direct rf feedback model.

A. Partial compensation

The cavity voltage amplitude $A_0(t)$ and phase $\phi_0(t)$ are calculated for constant generator current, magic detuning $\Delta\omega = \Delta\omega_m$, and optimal loaded quality factor $Q_L = Q_{L,opt}$. The reference signal is then

$$V_{ref}(t) = V_{cav} + (1 - k)[A_0(t)e^{i\phi_0(t)} - V_{cav}], \tag{34}$$

where k is the compensation factor. For $k = 0$, there is no compensation and no extra power is required for the generator during operation while the beam stability is maintained thanks to the reduction of cavity impedance Eq. (32). For $k = 1$ there is full compensation of the transient beam loading, which will come at a large cost in peak generator power.

B. Constant cavity voltage amplitude (LHC full detuning scheme)

As was discussed in Sec. II B, the aim is to keep the cavity voltage amplitude constant and minimize the peak generator power $\Delta\omega = \Delta\omega_{opt}$ and $Q_L = Q_{L,fd}$. Then the reference signal can be obtained from Eq. (29)

$$V_{ref,fd}(t) = V_{cav}\exp\left[-i\Delta\omega_{opt}\int_{t_0}^{t}\frac{A_b(u) - |F_b|I_{b,dc}}{|F_b|I_{b,dc}}du + i\phi(t_0)\right], \tag{35}$$

where $\phi(t_0)$ is adjusted to have a zero phase modulation averaged over a turn. As mentioned above this is a very good scheme for hadron colliders with $\phi_s \approx \pi/2$.

C. Constant cavity voltage amplitude and phase (LHC half-detuning scheme)

In proton machines with $\phi_s \approx \pi/2$ the half-detuning scheme was proposed in [21] that keeps the cavity voltage constant in amplitude and phase. Power consumption is minimum and the same in beam and no-beam segments for this scheme if the following cavity detuning and loaded quality factor are used:

$$\Delta\omega_{1/2} = -\omega_{rf}\frac{A_{b,peak}(R/Q)}{4V_{cav}}, \qquad Q_{L,1/2} = \frac{2V_{cav}}{(R/Q)A_{b,peak}}, \tag{36}$$

respectively. In this case the reference signal is constant

$$V_{ref,1/2}(t) = V_{cav}. \tag{37}$$

The LHC was operated in this mode until 2014.

IV. RESULTS AND COMPARISONS

This section presents the results of transient beam loading calculations for high-current future circular colliders. It is an extended version of the study presented in [22]. For the parameters of the FCC-ee Z with a variety of different filling schemes we present systematic comparisons of time-domain and frequency-domain approaches. Then, evaluation of the generator power during the ramp and transients at flat top for FCC-hh are discussed.

A. FCC-ee Z machine

We assume a constant generator current for evaluation of the beam induced transients (Sec. II A). To solve Eqs. (6)–(8), the Euler method is used with total calculation time longer than the cavity filling time ($\tau \approx 37$ μs), sufficient to get the steady-state solution. In the frequency-domain approach the Fourier image of the beam current modulation is multiplied by transfer functions [Eq. (24) with substitution $s = i\omega$] and then the inverse Fourier transform is used to obtain amplitude and phase modulations of the cavity voltage as well as the beam phase modulation. An example of a reasonable agreement of time-domain and frequency-domain calculations is shown in Fig 5. There is a strong modulation due to the abort gap and a finer structure due to the gaps between trains.

To study modulation of the beam and the cavity parameters systematically, the scan for different train

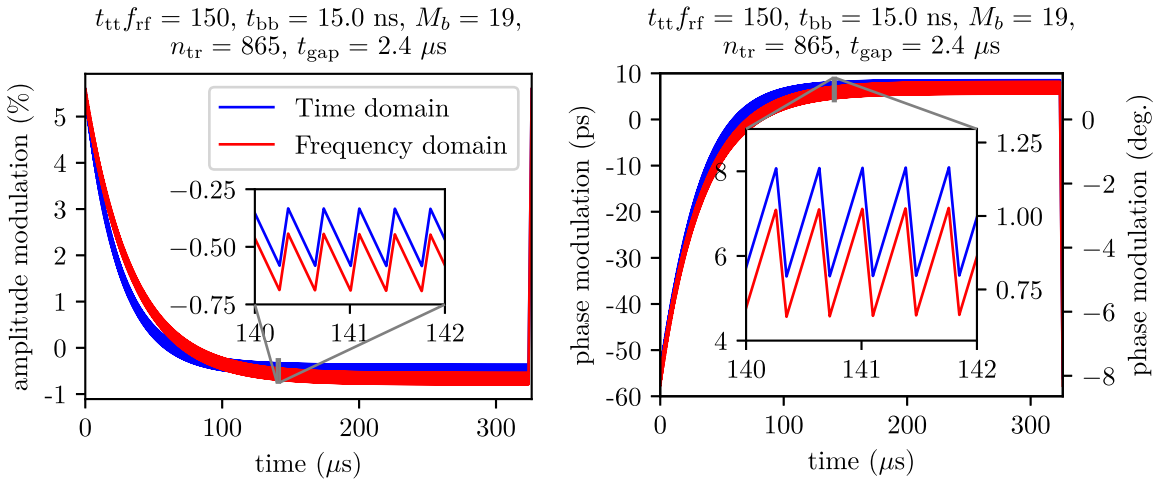

FIG. 5. Comparison of the time-domain [Eqs. (6)–(8)] and the frequency-domain approaches [Eqs. (24)] for the Z machine for magic detuning $\Delta\omega_m = \Delta\omega_{opt}/\sin^2\phi_s = 13.1$ kHz and the cavity filling time $\tau = 37$ μs. The figure shows the amplitude modulation of the cavity voltage (left) and the phase modulation of the cavity voltage (right) within one turn.

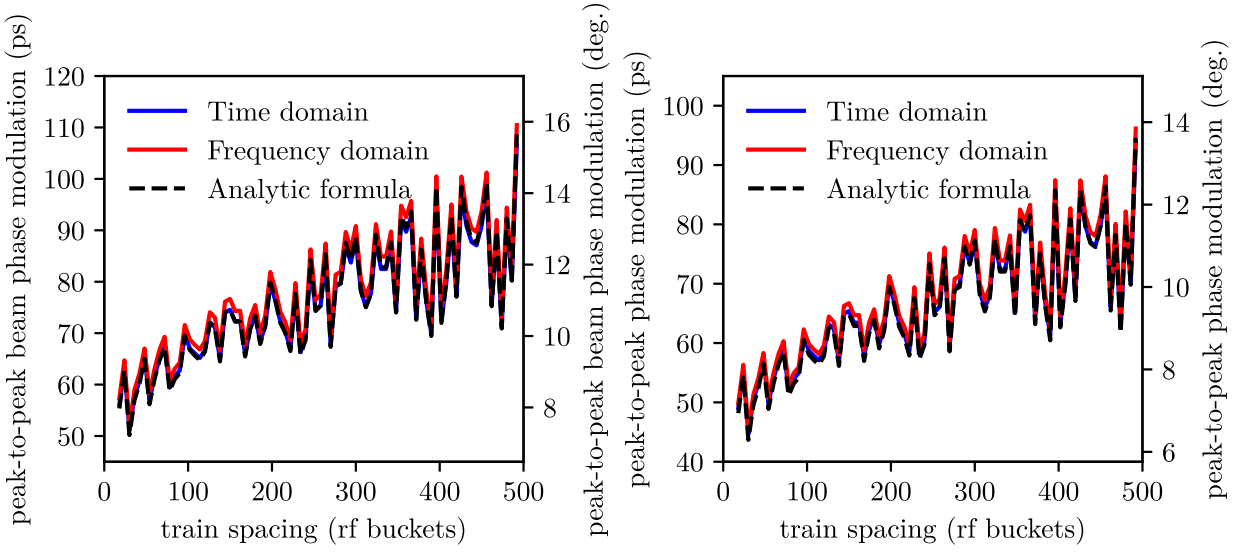

FIG. 6. Dependence of the peak-to-peak values for the beam phase modulation (left) and the phase modulation of the cavity voltage (right) on the train spacing for a bunch spacing of 15 ns. The results from the analytic formulas are given by Eq. (25) (left) and by Eq. (26) (right).

TABLE II. Examples of filling schemes used in Fig. 6.

Train spacing (rf buckets)	M_b	n_{tr}	M	t_{gap} (μs)
120	15	1082	16230	2.185
240	30	541	16230	2.260
360	46	360	16560	2.920
480	61	270	16470	2.995

spacings is performed for a fixed bunch spacing $t_{\mathrm{bb}} = 15$ ns and the maximum total number of bunches $M = 16640$ (Fig. 6). Examples of filling scheme used for calculations are listed in Table II. For each train spacing the peak-to-peak value of the beam phase modulation (the left-hand plot) and the phase modulation of the cavity voltage (the right-hand plot) are calculated. In general, the peak-to-peak values of phase modulations increase with larger train spacing because of longer abort gap. This comes from the fact that for larger t_{tt}, less bunch trains can circulate in the machine and it is more difficult to distribute them uniformly. For example, the abort gap will be the largest if the ring is filled with a single train. The results obtained in frequency domain are slightly larger than in the time domain. The difference is due to nonlinearities, which are accurately treated in time-domain calculations, while in the frequency-domain calculations they are neglected. The analytical formulas [Eqs. (25), (26)] agree very well with the results of the time-domain calculations (see the dashed black lines and the blue solid lines in Fig. 6, correspondingly). For $t_{\mathrm{tt}} f_{\mathrm{rf}} > 100$, the peak-to-peak beam phase modulation is larger than 70 ps, which corresponds to about 60 ps peak-to-peak phase modulation of the cavity voltage [the difference is the factor $1/\sin^2\phi_s$, see Eqs. (25) and (26)]. However, in operation, the shift of collision point can be minimized by matching abort gap transients. The dependence of the peak-to-peak phase modulation of the cavity voltage on the train spacing for different bunch spacings is shown in Fig. 7. In general, a larger bunch spacing leads to smaller transients because of more uniform filling that results in a shorter abort gap.

The comparison of amplitude modulations of the cavity voltage with the direct rf feedback ($\tau_d = 700$ ns, similar to the loop delay in the LHC [20]) for $k = 0.3$ and $k = 0$ [see Eq. (34)] is shown in Fig. 8. For partial compensation ($k = 0.3$) one can see about 15% reduction of the peak-to-peak value with about 10% increase of the instantaneous generator power (Fig. 9). Further optimizations with different filling schemes and parameters of the direct rf feedback can be performed to minimize transient beam loading in the FCC-ee Z. Note that the 10% increase in required power appears during the abort gap and the first few bunch trains (duration related to the rf feedback delay). It can thus be clamped (and reduced) with a tiny effect on the beam.

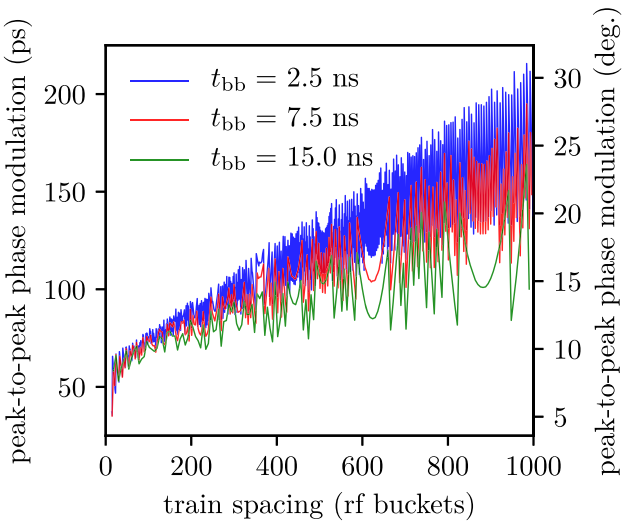

FIG. 7. Dependence of the peak-to-peak phase modulation of the cavity voltage from Eq. (26) on the train spacings for different bunch spacings.

B. Results for FCC-hh

The loss of Landau damping (LLD) in the longitudinal plane [3] is one of the limiting factors which defines the parameters of the FCC-hh rf system [2,23,24]. The proposed ramp lasts for 20 min and contains a linear part [region (ii) in Fig. 10] with 10% of parabolic parts at both ends [regions (i) and (iii) in Fig. 10]. The full longitudinal emittance and the filling factor q_p—the ratio of the maximum energy offset in the bunch to the bucket half-height—define the rf voltage for a given momentum program. The former increases with square root dependence on the beam energy (from 3.1 to 13 eVs) in order to be below the LLD threshold during the ramp. The latter is

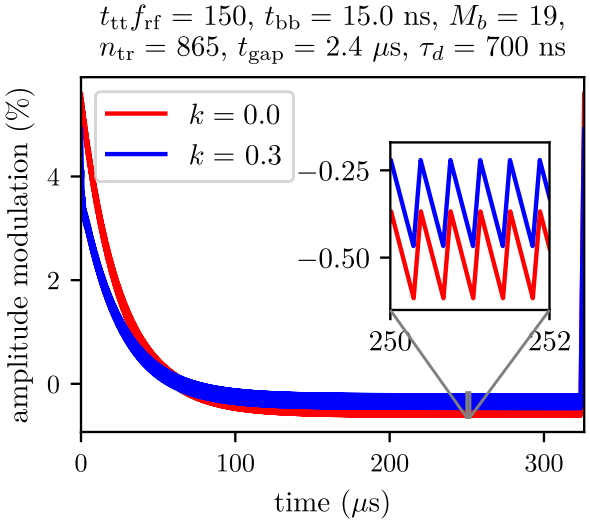

FIG. 8. Comparison of amplitude modulation of the cavity voltage with the direct rf feedback for different compensation factor k.

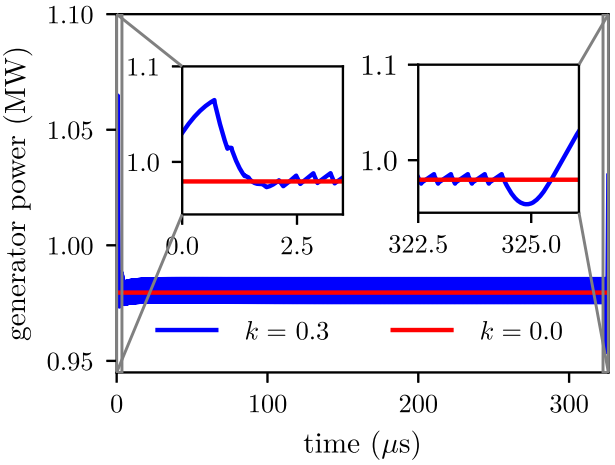

FIG. 9. Instantaneous generator power with the direct rf feedback for calculations shown in Fig. 8.

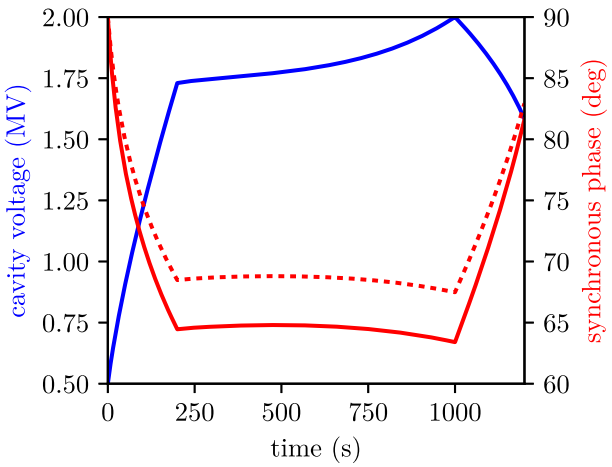

FIG. 11. Evolution of the cavity voltage, synchronous phase of the beam (red solid line), and the phase of the synchronous particle (red dotted line) during the ramp for the energy program and the filling factor shown in Fig. 10.

adjusted with linear and constant dependence on time to have the proper cavity voltage during the cycle which does not exceed 2 MV per cavity (see Fig. 10) [4].

The corresponding voltage program and synchronous phase as a function of time are shown in Fig. 11. The synchronous phase deviates from $\pi/2$ significantly during the ramp which means that the optimum detuning scheme could be an advantage in this case in terms of power consumption (Fig. 12). The synchronous phase differs from the phase of the synchronous particle as discussed in the Appendix. At the injection energy the half-detuning scheme will be used with $Q_L = 2.45 \times 10^4$ resulting in about 60 kW required peak generator power. To maintain cavity voltage amplitude and phase we assume the same total loop delay of the direct rf feedback $\tau_d = 700$ ns as in the LHC. After machine filling is done, the LHC full detuning scheme can be switched on and used for the initial stage of the ramp where the synchronous phase is close to $\pi/2$. In this region the quality factor increases linearly up to the value defined by Eq. (13). Then we propose to use the constant generator current scheme until the end of the ramp (no beam loading compensation) as it requires less generator power compared with the LHC full detuning scheme (see Fig. 12).

Comparing the results with the constant generator current at flat top for a single abort gap (8.65 μs) and four abort gaps (4×2.87 μs), the beam phase modulation is smaller for more uniformly distributed bunches, as expected (Fig. 13, left). It is less than 40 ps which is very small compared to the 1 ns long FCC-hh bunches. The peak-to-peak cavity voltage amplitude modulations for both cases are smaller than 4% (Fig. 13, right) and produce bunch length modulations that are negligible compared with the natural spread between bunches (about 5% in

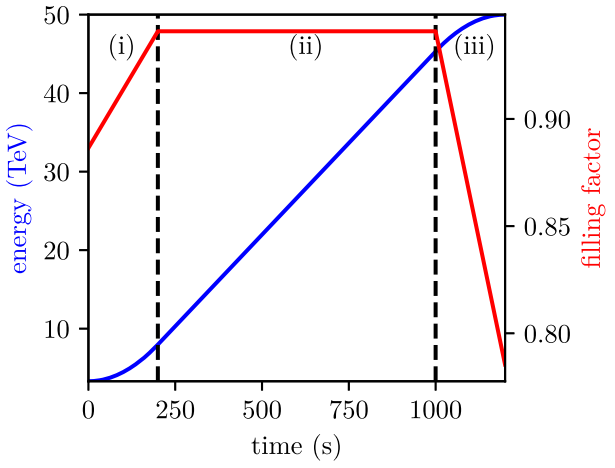

FIG. 10. The energy program and evolution of the filling factor during the ramp in the FCC-hh: (i) the parabolic, (ii) linear, and (iii) parabolic parts of the energy program.

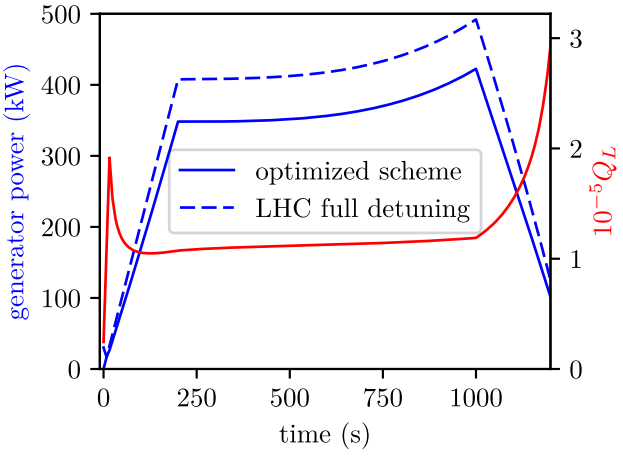

FIG. 12. Evolution of the generator power and the loaded quality factor during the ramp for the energy program and the filling factor shown in Fig. 10.

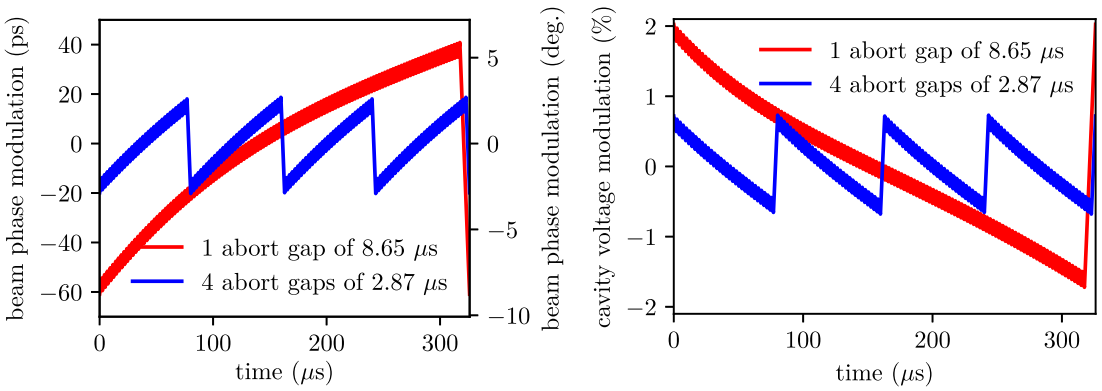

FIG. 13. Modulations of the beam phase (left) and of the cavity voltage amplitude (right) at flat top in FCC-hh for different abort gap configurations and constant generator current.

the LHC). This means that the FCC-hh can be operated at the flat top with magic detuning $\Delta\omega_m = -4.7$ kHz, optimal loaded quality factor $Q_{L,\mathrm{opt}} = 3 \times 10^5$, and about 102 kW input power keeping the generator drive constant.

We also realized that for the cases of larger phase modulations of the cavity voltage (above 20°) the system of Eqs. (6)–(8) becomes unstable. This indicates that the Robinson stability criterion could be different for the case of large transients. However, the beam remains stable even for the optimal parameters in the presence of the direct rf feedback (see for example [25]).

V. CONCLUSIONS

In the present work the beam loading in high-current future circular colliders has been analyzed. We have shown that the equations of frequency-domain analysis can be obtained by linearization of the more accurate time-domain equations that are valid for any values of the beam current modulations.

For the assumed regular filling schemes, the main contribution to the phase and amplitude modulations of the cavity voltage comes from the abort gap. For the FCC-ee Z the resulting peak-to-peak value of the bunch-by-bunch phase modulation is larger than 70 ps for an abort gap longer than 2 μs. The larger train spacings lead to stronger modulation of cavity and beam parameters, which can be reduced by using filling schemes with larger bunch spacings. The direct rf feedback can mitigate the transient beam loading at the cost of additional generator power. For the overall loop delay $\tau_d = 700$ ns, about 10% increase of the peak generator power is sufficient to reduce the peak-to-peak amplitude modulation of the cavity voltage by 15%.

In the FCC-hh the magic detuning without transient beam loading compensation should be used during the ramp. Transient beam loading compensation schemes demand very large peak power because the synchronous phase differs significantly from $\pi/2$. Without compensation, the maximum generator power during acceleration is about 420 kW and at flat top it is slightly above 100 kW. With four distributed abort gaps the peak-to-peak values of the beam phase modulation and the cavity voltage amplitude modulation are less than 40 ps and 2%, respectively. This means that the FCC-hh can be operated without transient beam loading compensation at the collision energy.

This paper has derived power requirements based on the beam-cavity-generator interaction at the fundamental mode, described in Eq. (2). The rf component of the beam current is considered as an external "perturbation". Further studies should focus on development of a model including both longitudinal dynamics (the action of cavity voltage on the beam) and hardware limitations (such as nonlinearity of the generator, limited bandwidth of the power parts, misalignments of the low level rf and tune settings, rf noise, etc.), similar to the studies done for PEPII [8] and the LHC [26]. A possible impact of mismatched transients on luminosity depending on the collision scheme of both FCC-ee and FCC-hh needs to be also addressed.

ACKNOWLEDGMENTS

We thank Elena Shaposhnikova, Dmitry Teytelman, Rama Calaga, Andrew Butterworth, Alessandro Gallo, and Olivier Brunner for useful discussions and comments.

APPENDIX: LINE DENSITY CALCULATION

For the case of a single rf system with a sinusoidal rf wave, the Hamiltonian is

$$H(\epsilon, \varphi) = \frac{h\eta}{2\beta^2 E_s}\epsilon^2 + \frac{eV_{\mathrm{tot}}}{2\pi}W(\varphi). \tag{A1}$$

Here $\epsilon = E_p - E$ energy offset of the particle with respect to the energy of the synchronous particle E, h is the harmonic number, $\eta = \alpha_p - 1/\gamma^2$ is the slip factor, and V_{tot} is the total rf voltage. The normalized rf potential W is defined as

$$W(\varphi) = \sin\phi_{s0} - \sin\varphi - (\phi_{s0} - \varphi)\cos\phi_{s0}, \tag{A2}$$

where the phase of the synchronous particle (electron machine convention) is

$$\phi_{s0} = \arccos\left(\frac{U_0 + \Delta E}{eV_{\mathrm{tot}}}\right) \tag{A3}$$

so that at each turn the rf cavities give a momentum kick, which compensates the energy loss due to synchrotron radiation U_0 and produces acceleration with the energy gradient ΔE. In the present work we assume the binomial particle distribution as a function of Hamiltonian

$$\psi[H(\epsilon,\varphi)] = \psi_0[H_{\mathrm{max}} - H(\epsilon,\varphi)]^{\mu}, \tag{A4}$$

where ψ_0 is the normalization constant, and $H_{\mathrm{max}} = eV_{\mathrm{tot}}W_{\mathrm{max}}/(2\pi)$ is the Hamiltonian of the particle with the maximum energy offset, and W_{max} is the corresponding value of the rf potential. In the LHC $\mu \approx 2$ and it is assumed to be $\mu = 1.5$ for proton bunches in the FCC-hh because continuous emittance blow-up is applied during the ramp and at flat top resulting in flatter bunches. For $\mu \gg 1$ the distribution becomes Gaussian, which is the case for electron bunches in the FCC-ee. After integration over ϵ one gets the line density [27]

$$\lambda(\varphi) = \lambda_0[W_{\mathrm{max}} - W(\varphi)]^{\mu+\frac{1}{2}} \tag{A5}$$

with λ_0 the normalization constant. Finally, the complex form factor can be obtained using Eq. (4). For short FCC-ee bunches $|F_b| \approx 2\exp[-(\omega_{\mathrm{rf}}\sigma)^2/2]$ and $\phi_s \approx \phi_{s0}$, while for long FCC-hh bunches the bunch shape asymmetry is significant, so that the synchronous phase of the bunch differs from one of the synchronous particle (see Fig. 11).

[1] A. Abada *et al.*, FCC-ee: The Lepton Collider, Eur. Phys. J. Spec. Top. **228**, 261 (2019).

[2] A. Abada *et al.*, FCC-hh: The Hadron Collider, Eur. Phys. J. Spec. Top. **228**, 755 (2019).

[3] F. J. Sacherer, A longitudinal stability criterion for bunched beams, IEEE Trans. Nucl. Sci. **20**, 825 (1973).

[4] I. Karpov and E. Shaposhnikova, in *The fifth Annual Meeting of the Future Circular Collider Study, Brussels* (2019), https://indico.cern.ch/event/727555/contributions/3439881/attachments/1868115/3073133/Beam_dyn_and_RF_IK_ES.pdf.

[5] F. Pedersen, Beam loading effects in the CERN PS booster, IEEE Trans. Nucl. Sci. **22**, 1906 (1975).

[6] D. Teytelman, *The Third Annual Meeting of the Future Circular Collider Study, Berlin* (2017), https://indico.cern.ch/event/556692/contributions/2590414/attachments/1468181/2271216/3WE16C.pdf.

[7] J. M. Byrd, S. De Santis, J. Jacob, and V. Serriere, Transient beam loading effects in harmonic rf systems for light sources, Phys. Rev. ST Accel. Beams **5**, 092001 (2002).

[8] C. Rivetta, T. Mastorides, J. D. Fox, D. Teytelman, and D. Van Winkle, Modeling and simulation of longitudinal dynamics for Low Energy Ring–High Energy Ring at the Positron-Electron Project, Phys. Rev. ST Accel. Beams **10**, 022801 (2007).

[9] J. Tückmantel, CERN Report No. CERN-ATS-Note-2011-002 TECH, 2011, https://cds.cern.ch/record/1323893/files/CERN-ATS-Note-2011-002%20TECH.pdf.

[10] T. Mastoridis, P. Baudrenghien, and J. Molendijk, Cavity voltage phase modulation to reduce the high-luminosity Large Hadron Collider rf power requirements, Phys. Rev. Accel. Beams **20**, 101003 (2017).

[11] I. Karpov, R. Calaga, and E. Shaposhnikova, High order mode power loss evaluation in future circular electron-positron collider cavities, Phys. Rev. Accel. Beams **21**, 071001 (2018).

[12] E. Renner, M. J. Barnes, W. Bartmann, F. Burkart, E. Carlier, L. Ducimetière, B. Goddard, T. Kramer, A. Lechner, N. Magnin, V. Senaj, J. Uythoven, P. V. Trappen, and C. Wiesner, in *Proceedings of the 9th International Particle Accelerator Conference, Vancouver, British Columbia, Canada* (2018), pp. 10–13, http://ipac2018.vrws.de/papers/tupaf058.pdf.

[13] P. F. Tavares, A. Andersson, A. Hansson, and J. Breunlin, Equilibrium bunch density distribution with passive harmonic cavities in a storage ring, Phys. Rev. ST Accel. Beams **17**, 064401 (2014).

[14] K. W. Robinson, Report No. CEAL-1010, 1964, https://www.osti.gov/biblio/4075988.

[15] Y is the ratio of the beam induced voltage with cavity on tune (and no generator current) to the desired V_{cav} [14].

[16] F. Pedersen, CERN Report No. CERN-PS-92-59-RF, 1992, https://cds.cern.ch/record/244817.

[17] D. Boussard, in *Handbook of Accelerator Physics and Engineering*, 2nd ed. (World Scientific, Singapore, 2013), p. 131, https://www.worldscientific.com/doi/pdf/10.1142/8543.

[18] D. Boussard, in *Proceedings of 1991 IEEE Particle Accelerator Conference (APS Beam Physics)* (1991), p. 2447, https://cds.cern.ch/record/221476/files/cer-000134053.pdf.

[19] D. Boussard, Control of cavities with high beam loading, IEEE Trans. Nucl. Sci. **32**, 1852 (1985).

[20] P. Baudrenghien and T. Mastoridis, Fundamental cavity impedance and longitudinal coupled-bunch instabilities at the High Luminosity Large Hadron Collider, Phys. Rev. Accel. Beams **20**, 011004 (2017).

[21] D. Boussard, CERN Report No. CERN-SL-91-16-RFS, 1991, https://cds.cern.ch/record/221153.

[22] I. Karpov and P. Baudrenghien, in *Proceedings of 61st ICFA Advanced Beam Dynamics Workshop (HB 2018), Daejeon, Korea* (JACoW Publishing, Geneva, 2018), pp. 266–271, https://doi.org/10.18429/JACoW-HB2018-WEP2PO003.

[23] E. Shaposhnikova, in *The Third Annual Meeting of the Future Circular Collider Study, Berlin* (2017), https://indico.cern.ch/event/556692/contributions/2484257/attachments/1467380/2269248/FCChh_RF_Berlin.pdf.

[24] E. Shaposhnikova and I. Karpov, *The Fourth Annual Meeting of the Future Circular Collider Study, Amsterdam* (2018), https://indico.cern.ch/event/656491/contributions/2930759/attachments/1631764/2602214/FCC_Week_2018_Shaposhnikova_Karpov.pdf.

[25] A. Mosnier, F. Orsini, and B. Phung, in *Proceedings of the 6th European Particle Accelerator Conference (EPAC'98), Stockholm, Sweden* (1998), http://accelconf.web.cern.ch/Accelconf/e98/PAPERS/WEP28G.PDF.

[26] T. Mastorides, C. Rivetta, J. D. Fox, D. V. Winkle, and P. Baudrenghien, RF system models for the CERN Large Hadron Collider with application to longitudinal dynamics, Phys. Rev. ST Accel. Beams **13**, 102801 (2010).

[27] T. Linnecar and E. N. Shaposhnikova, CERN Report No. SL-Note-92-44-RFS, 1992, https://cds.cern.ch/record/703261.